# Circular DNA Molecules Imaged in Air by Scanning Force Microscopy†

Carlos Bustamante,*,‡ James Vesenka,‡ Chun Lin Tang,‡ William Rees,‡ Martin Guthold,‡ and Rebecca Keller§
*Institute of Molecular Biology and Department of Chemistry, University of Oregon, Eugene, Oregon 97403, and Department of Chemistry, University of New Mexico, Albuquerque, New Mexico 87413*
*Received October 11, 1991*

ABSTRACT: Routine and reproducible imaging of DNA molecules in air with the scanning force microscope (SFM) has been accomplished. Circular molecules of plasmid DNA were deposited onto red mica and imaged under various relative humidities. In related experiments, the first images of the *Escherichia coli* RNA polymerase–DNA complex have also been obtained. This has been possible by (1) the use of specially modified SFM tips with a consistent radius of curvature of 10 nm or less, to minimize the amount of image distortion introduced by the finite dimensions of commercially available tips, (2) the optimization of a method to deposit and bind DNA molecules to the mica surface in a stable fashion, and (3) careful control of the sample humidity, to prevent solvation of the molecules and detachment from the surface by the scanning tip or stylus. Contact forces in the range of a few nanonewtons are routinely possible in air and in the presence of residual humidity. The spatial resolution of the images appears determined by the radius of curvature of the modified styli, which can be estimated directly from the apparent widths of the DNA molecules in the images.

Scanning probe microscopies are based on the ability to detect a local property of a surface by means of a spatially controlled sensor or probe (Hansma et al., 1988; Rugar & Hansma, 1990). Typically, the probe is scanned over the area of interest so it is only transiently localized in the neighborhood of a given point on the surface. The spatial distribution of the magnitude of the quantity measured on the surface provides a position-dependent signal or "image" of the surface. Depending on the sensor and the mode of operation, images depict the topography, the electronic structure, or the mechanical or thermal properties of the surface. The spatial resolution of these methods is critically dependent on the property measured and the type of interaction between the probe and the surface. The two most common techniques are the scanning tunneling microscopy (STM) and the scanning force microscopy (SFM). The SFM uses a sensor tip carried by a cantilever with a small spring constant (Binnig et al., 1986). The atomic-scale topography of the sample is obtained by recording the angstrom displacements of the cantilever as the object is scanned past the tip. The displacement can be detected by shining a laser on the back of the cantilever to record the deflection of the reflected beam on a light-sensitive diode. The measured deflection is proportional to the force between the surface and the tip. Commercial cantilevers are microfabricated from $Si_3N_4$, Si, or $SiO_2$ and have typical spring constants between 0.1 and 1.0 N/m. For comparison, the spring constant between two atoms is about 10 nN/m (Rugar & Hansma, 1990).

The SFM has many distinct advantages over other forms of microscopy, the most important being its ability to operate, unlike the STM, on nonconductive samples and under physiologically relevant conditions, making it easier to use with a biological specimen. Several reports have appeared during the last 3 years on the applications of SFM to the direct visualization of biological molecules. For a recent review, see Engel (1991). Images of DNA have been reported in the literature (Lindsay et al., 1989; Weisenhorn et al., 1990; Hansma et al., 1991), but results have shown poor reproducibility. These problems result from (1) lack of a suitably flat, strongly adsorbing substrate, (2) less than optimal tip–molecule interactions, (3) lack of consistently sharp styli, and (4) the need to develop optimal ambient conditions for imaging.

In this paper we present results of work designed to address these problems. It will be shown that the crucial aspect affecting the imaging reproducibility of biological samples in air is the lack of suitably sharp styli. Using tips especially modified by an electron beam to give styli with a radius of curvature of about 10 nm, circular DNA molecules can be imaged in air routinely. Use of these consistently sharp styli has allowed us to develop a simple method to firmly bind DNA to mica in air. Moreover, it will be shown that if these sharp styli are used on samples under relative humidity control, the stylus–molecule forces can be easily minimized, and a range of stylus–sample forces can be utilized without inducing sample damage. This method is also used here to image restriction fragments of DNA and the *Escherichia coli* RNA polymerase–DNA complex. The subtle interplay between tip dimensions and water capillary forces which participate in SFM imaging of biological samples in air is discussed.

## Materials and Methods

The DNA plasmids DL34 (Lazinski et al., 1989), VCB5 (DeLange et al., 1986), and SK31 were dissolved in a buffer of 10 mM Tris, pH 7.6, and 1 mM EDTA. Plasmid SK31 (pSK31) and fragments of pSK14 and pSK16 are derived from pWW31, pWW14, and pWW16 (Whalen et al., 1988). pSK31 and pSK16 were constructed by inserting the *Eco*O109–*Hin*dIII fragments from pWW16 and pWW31, respectively, into the plasmid $pSK^+$ (Stratagene, La Jolla, CA) that had been digested with the same restriction enzymes. pSK14 was constructed by inserting the *Kpn*I–*Hin*dIII fragment from pWW14 into *Kpn*I–*Hin*dIII digested $pSK^+$. All three restriction fragments from the WW plasmids contain the λ $P_L$ promoter upstream of the ρ-independent transcription terminator tR′.

pRB2 was constructed as follows: The *Eco*O109–$P_L$–*Eco*RI fragment from pWW10 (Whalen et al., 1988) was ligated with the large fragment of $pSK^+$ after removal of the small *Eco*O109–*Eco*RI fragment, to form pRB1. pRB1 was line-

† This work is partially supported by NIH Grant GM 32543, NSF Grant DIR-8820732 to C.B., and the Lucille P. Markey Charitable Trust to the Institute of Molecular Biology, University of Oregon.
* To whom correspondence should be addressed.
‡ University of Oregon.
§ University of New Mexico.

0006-2960/92/0431-22$03.00/0 

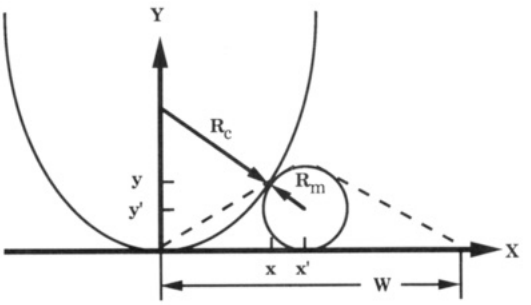


FIGURE 1: Schematic of tip/surface/biomolecule contact. All surfaces are assumed to be rigid. As the tip, of radius $R_c$, scans the biomolecule, of radius $R_m$, the image width, $W$, is recorded by the microscope software.

arized by digestion with *Pst*I and *Xba*I, and the *Pst*I–tR′–*Xba*I fragment from pDL11 was inserted to generate pRB2. DNA plasmid fragments complexed with RNA polymerase are constructed by the method of Levin et al. (1987).

Red mica (Ashville-Schoonmacher) is freshly cleaved and briefly sonicated in deionized/distilled water. The mica is then soaked in 33 mM magnesium acetate overnight to favor the replacement of potassium ions by magnesium in the mica surface so as to provide a stronger binding site with the phosphate groups of the DNA. The mica is then sonicated for 30 min in distilled water to remove the buildup of excess salts on the surface, providing a smooth substrate for observing the biomolecules. The mica surface is glow discharged for 15 s in a vacuum between 100 and 200 mTorr, a process that hardens the substrate and imparts a hydrophilic surface. As soon as the substrate is brought up to air, a few microliters of 10 μg/mL DNA solution is deposited on the surface and allowed to absorb for 2 min. The sample is then rinsed with water and blown dry with nitrogen (Vesenka et al., 1992).

The specimens were imaged with a Digital Instruments Nanoscope II scanning force microscope and software. All samples were imaged in air at room temperature, in the attractive force regime and under conditions of controlled relative humidity typically in the range of 30–60%. Force minimization was maintained by reducing the "set point voltage" (withdrawing the piezo from the tip) in order to minimize sample damage. Only minimal filtering to remove the high-frequency noise in the slow scan direction was applied to the images.

Only commercially available ($Si_3N_4$) cantilevers with spring constants of about 0.1 N/m were used in this work. The tetrahedral tips attached to these cantilevers were modified under a beam of an electron microscope, following a procedure reported previously (Lee et al., 1989; Akama et al., 1990; Keller & Chih-Chung, 1991). The method utilizes the fact that contaminating vacuum pump hydrocarbons can be selectively deposited by the electron beam in the form of a carbonized material on the apex of commercially available tips, yielding sharper "microtips" or styli, with a radius of curvature of about 10 nm.

In scanning force microscopy, the finite dimensions of the tips introduce a lateral deformation of the objects imaged. For the imaging geometry shown in Figure 1, involving a parabolic tip with a radius of curvature $R_c$ imaging a molecule with a molecular radius $R_m$, the apparent width of the molecule $W$ is given by

$$W = \frac{4(R_c + R_m)\sqrt{R_m(R_c - R_m)}}{R_c}, \quad R_c > R_m \qquad (1)$$

This expression can be used to predict the width of a molecule for a given radius of curvature of the tip. More importantly, as will be shown here, having demonstrated the reliability and reproducibility of DNA imaging, eq 1 can be used to estimate the dimensions of the radius of curvature of the styli from the actual and imaged widths of DNA.

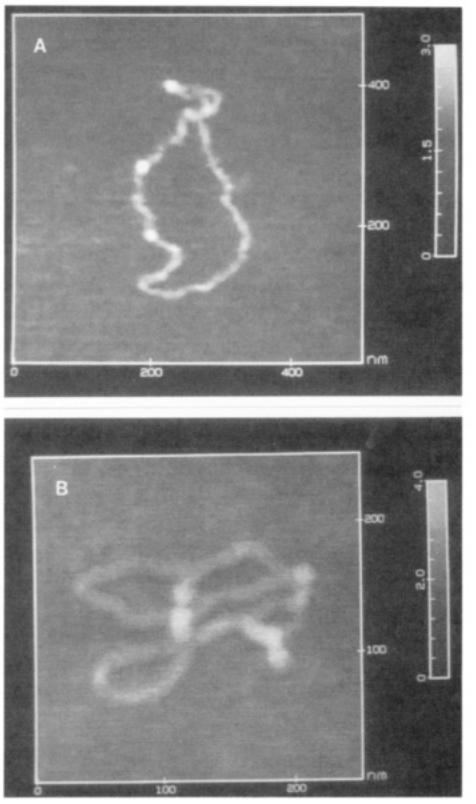


FIGURE 2: SFM images in air of a 3-kbp plasmid attached to the surface of magnesium acetate soaked, glow-discharged mica. The plasmid is easily distinguished from the background, and it is 940 nm long, 12 nm wide, and about 1.0 nm tall.

## Results

*Imaging of Plasmid Molecules.* Panels A and B of Figure 2 are typical images of a 3.3-kbp plasmid DNA obtained at 30% relative humidity and a force of about 3 nN. At this humidity, plasmid molecules were scanned for several hours without damaging the samples, even when imaging at higher magnifications. The lengths, widths, and heights of three relaxed plasmid samples were measured and are shown in Table I. The lengths of these plasmids were all within the range expected for molecules that are partly or completely converted to the A form at the humidities used in these experiments (Pilet & Brahms, 1972). The average height of the DNA images was 1.32 ± 0.35 nm. All heights were measured as the difference between the top of the biomolecules and the average height of the underlying substrate. The image widths were measured from sample/substrate contact points on each side of the biomolecule and varied depending on the stylus used and the sample studied. The average width value in these studies was 12.3 ± 3.3 nm.

*Effect of Relative Humidity.* Figure 3 illustrates the effect of high relative humidity (rh) on the imaging of DNA plasmids. Three successive images obtained at 65% rh and 10-nN force are shown. The repeated scanning of the tip over the molecule moves the molecule from side to side slightly at first (panel A) and then more pronouncedly (panels B and C). By the fourth image the plasmid disappeared, swept aside by the stylus. These effects could be avoided by imaging the molecules below 45% rh.

*Imaging of Restriction DNA Fragments and RNA POL–DNA Complexes.* Having demonstrated the possibility of

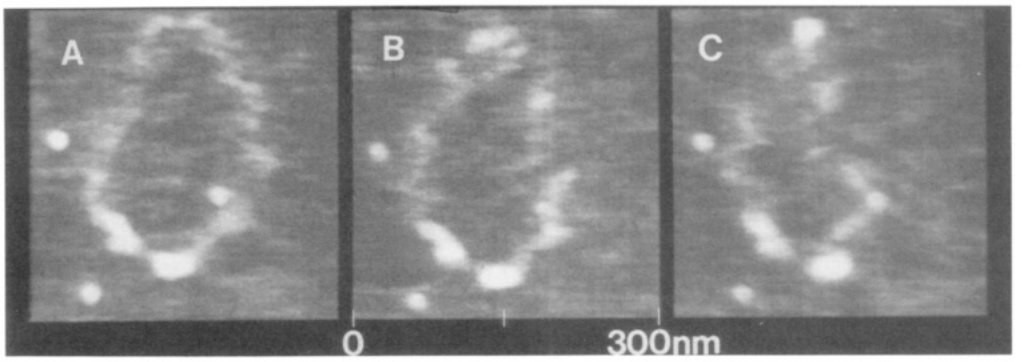


FIGURE 3: Sequence of scanning images of a 3-kbp plasmid at 65% humidity. With each successive scan the plasmid becomes more detached from the substrate. The vertical scale is the same as in Figure 2A.

Table I

| DNA | calculated length (nm)[a] | measured length (nm) | measured height (nm) | measured width (nm) |
|---|---|---|---|---|
| pDL34[b] | 880–1069 | 1049 ± 52 | 0.65 ± 0.26 | 13.1 ± 4.3 |
| pVCB5[c] | 823–1000 | 874 ± 54 | 1.89 ± 0.72 | 10.3 ± 3.4 |
| pSK31[d] | 930–1130 | 938 ± 35 | 1.43 ± 0.09 | 12.7 ± 2.2 |
| fSK14[e] | 174–211 | 93 ± 23 | 1.22 ± 0.18 | 9.4 ± 1.5 |
| fRB2[f] | 144–175 | 117 ± 37 | 1.60 ± 0.18 | 12.9 ± 2.7 |
| complex[g] | 129–156 | 100 ± 18 | 1.73 ± 0.30 | 13.1 ± 0.4 |
| fSK16[h] | 156–190 | 169 ± 13 | 0.89 ± 0.20 | 13.1 ± 1.7 |
| complex[i] | 130–157 | 160 ± 23 | 0.98 ± 0.18 | 13.2 ± 2.0 |

[a] Length calculated by assuming a conformational change of 0.34–0.28 nm per base pair (B → A) at reduced humidity (Pilet & Brahms, 1972). [b] Average of seven plasmid images at 45% relative humidity (rh). [c] Average of five plasmid images at 60% rh. [d] Average of eight plasmid images at 30% rh. [e] Average of ten fragment images at 30% rh. [f] Average of nine fragment images at 30% rh. [g] Average of nine RB2.5 fragment/RNAp complex images with an RNAp height of 1.22 ± 2.1 nm and width of 28.6 ± 8.0 nm at 30% rh. [h] Average of three fragment images at 30% rh. [i] Average of three SK16 fragment/RNAp complex images with an RNAp height of 2.65 ± 0.17 nm and width of 31.0 ± 6.6 nm at 30% rh.

imaging DNA molecules in a routine fashion, an attempt was made to exploit the small radii of curvature of the modified styli to image small DNA fragments. Figure 4A shows an image of the DNA restriction fragment fSK14, 623 bp long, obtained with a force of 3 nN. The length, height, and width of these molecules was 110 nm, 1.15 nm, and 6.8 nm, respectively. Assuming a molecular radius of 1 nm and the above width, a radius of curvature of 2.9 nm for the stylus used in this image can be estimated using eq 1. However, because of the compression experienced by the molecules illustrated by a 40% reduction in height, this value is most likely a lower limit. Using the deformed height, a more realistic figure for the radius of curvature of the tip is ~5 nm. In total, ten fragments were imaged and their lengths, heights, and widths were measured. The values are shown in Table I.

The next step was to test the feasibility of imaging DNA–protein complexes under the SFM. To this end, the plasmid fragment fSK16, 463 bp long, carrying a T7 promoter located about two-fifths from one end of the molecule, was reacted with RNA polymerase I. The complexes were formed under conditions in which the polymerase was added either in equimolar or in some excess quantities relative to the promoter-carrying fragments. Figure 4B shows an image of one of these transcription complexes. The fragments show a characteristic widening slightly off the center of the DNA fragment, as expected. Because these observations were systematic, the enlargement was identified with the polymerase molecule. The average height, width, and length of the DNA fragment is 0.98 ± 0.18 nm, 13.2 ± 2.0 nm, and 162 ± 23 nm, respectively. The height and width of the polymerase region

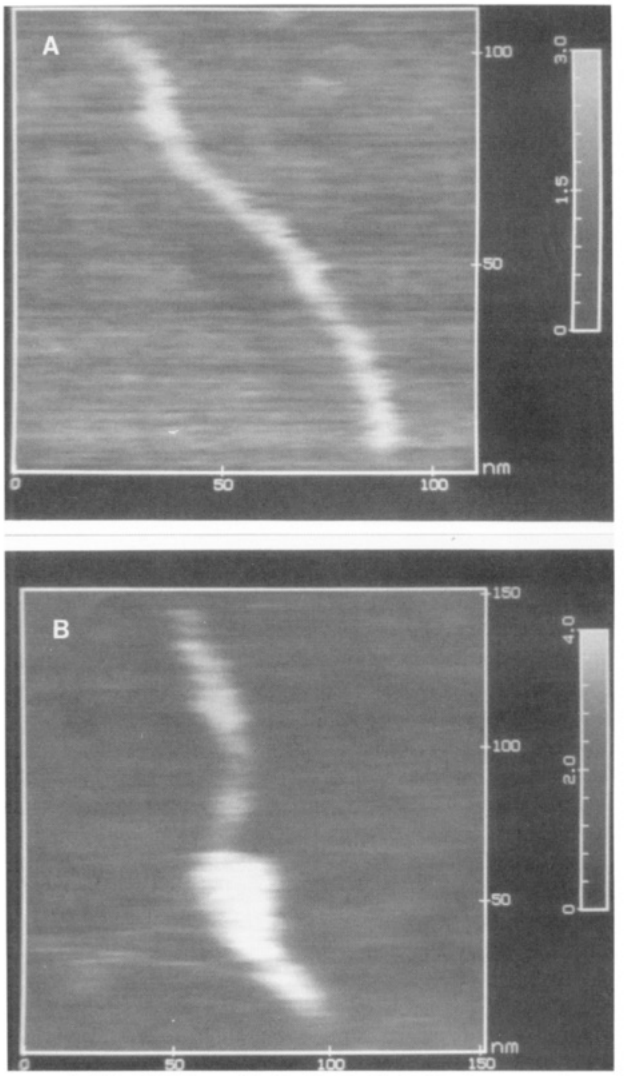


FIGURE 4: (A) SFM image in air of a 514-bp DNA fragment, imaged under a load force of 3 nN. (B) SFM image under air of an RNA polymerase complex with the plasmid DNA fragment carrying a bacteriophage T7 promoter.

is 1.22 ± 0.21 nm and 28.6 ± 8.0 nm, respectively.

*Effect of the Loading Force.* Figure 5 shows the effect of the loading force on the imaging of a plasmid DNA molecule. The first image was obtained at the intermediate force of 20 nN. Many scans were obtained without affecting the plasmid, although the molecule appears somewhat flattened (the height at the arrow in a coiled region is 1.01 nm and the width is 2.1 nm), but the distorsion is not too large. At 110 nN, the molecule is beginning to appear distorted (the height at the arrow is 0.62 nm and the width is 29 nm). At a force of 170

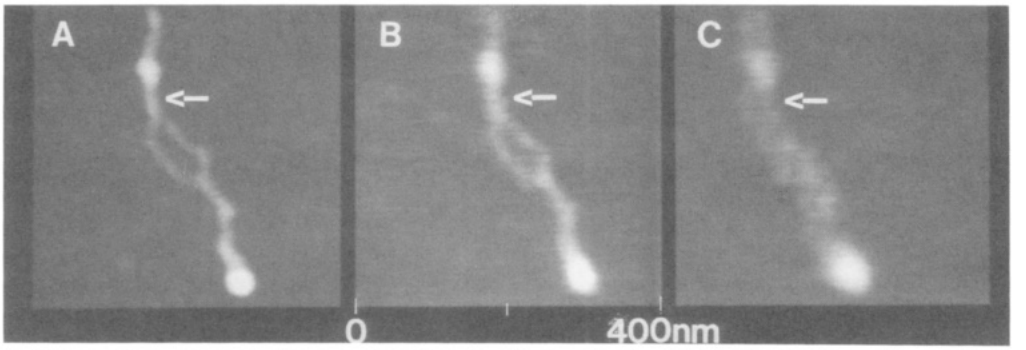


FIGURE 5: A series of images illustrating the effect on a plasmid molecule of progressively higher loading forces. All the images were obtained at 45% relative humidity. See text for explanation. The vertical scale is the same as in Figure 4A.

nN the molecule has been smashed by the loading force, and moreover, the damage appears irreversible since the original image was not recovered when the force was reduced back to its initial value. By the end of this process the height had reduced to 0.49 nm and the width increased to 47 nm. Details discussing the use of the SFM stylus for dissecting plasmid DNA are given in Vesenka et al. (1992).

## Discussion

These results represent the first systematic and reproducible imaging of DNA molecules by the scanning force microscope. Routine imaging of the samples discussed above has been possible by the use of electron-beam-deposited styli with radii of curvature 3–5 times smaller than those of commercially available tips. The use of sharper tips in SFM imaging in air has two main effects: (1) a decrease of the liquid–air interface at the point of contact between the tip and the sample and (2) a reduction of the lateral distortion in the images, introduced by the finite dimensions of the tips.

In the absence of capillary forces, a parabolically shaped tip in contact with a flat surface will be subject to van der Waals forces proportional to $R_c/d$, where $R_c$ is the radius of curvature of the tip and $d$ is the distance between the tip and the sample (Keller, private communication). When samples are imaged in air, a water layer of varying thickness is present on the sample. In these conditions, the aqueous meniscus formed between the tip and the sample induces capillary forces that scale with the radius of curvature of the tip. Thus, in air, the forces involved in the SFM experiment are usually higher than those estimated from pure van der Waals considerations (Persson, 1987). As a result, using sharper tips will generally minimize the dimensions of the air–liquid interphase, making it possible to operate at lower forces, which are, in turn, easier to control. An order of magnitude calculation supports this interpretation. It has been reported that attractive capillary forces of 400 nN develop between the tip and the surface of mica, when imaging is performed in air without humidity control and when commercially available tips are used (Weisenhorn et al., 1989). Since the capillary force is also proportional to $R_c$, a reduction in this parameter by a factor of 5 would result in a force of the order of $10^{-8}$ N. When the relative humidity is decreased to 30% or 40%, forces closer to $10^{-9}$ N, as observed here, can be routinely obtained.

The spatial resolution of the scanning force microscope is determined by the shape and dimensions of the tip. The effect of a blunt tip is to deform the lateral dimensions of the object. Commercially available pyramidal-shaped silicon nitride tips ($Si_3N_4$) are microfabricated from a silicon template with radii of curvature of between 40 and 50 nm. These dimensions are huge compared to the lateral dimensions of most biomolecules and effectively limit the spatial resolution of the SFM. Images of DNA reportedly with 2–6-nm widths have been obtained with commercial tips, but not reproducibly (Henderson, private communication) and are likely to be the fortuitous result of microtip defects at the end of the styli (Zasadzinski et al., 1991).

Furthermore, we were never successful at imaging DNA on the magnesium-treated mica substrate in air with commercial tips. Tip engagement was always accompanied with excessive vertical noise (>1 nm) preventing imaging. We suspect this might have been caused by charge buildup between two electrically insulating surfaces ($Si_3N_4$ and mica), interfering with continuous surface contact. In fact, gold/palladium-sputtered tips could be used to image DNA and only occasionally yielded the lateral dimensions obtained with electron-beam-deposited tips. It is possible that metal sputtering both provides a small defect at the tip's end and prevents charge buildup. Use of sharper electron-beam-deposited tips greatly reduces lateral image distortion and simplifies the recognition of the deposited molecules.

Scanning at low forces was possible at relative humidities of 40% or less. It appears that above 60% relative humidity, molecule–tip interactions become comparable to those binding the molecule to the mica surface, allowing the stylus to detach and sweep the molecules during the scan. The molecular mechanism of this process is not yet clear, but it is likely that at higher humidities the thickness of the water layer condensed on the surface increases, leading to either or both of two effects: (1) partial solvation of the molecule from the surface due to the screening of the electrostatic charges holding the molecule down and (2) an increase in molecule–tip interaction due to enhanced surface tension effects. These effects restrict the range of conditions adequate for imaging these molecules using the methods described here. A further solution of this limitation might involve the development of methods of chemical attachment of the macromolecules to the surface that will not be severely weakened by water condensation. Such methods could presumably also work for imaging under water, with the benefit of eliminating the air–liquid interphase and the influence of the surface tension.

The images depicting the DNA–RNA polymerase complexes show the protein flattened comparatively more than the DNA molecule. This is to be expected, for proteins are less resistant than DNA to dehydration. When the polymerase was added in some excess with respect to the DNA, often the enlargement along the fragment was observed at one of its ends, the site of strong unspecific binding.

The images obtained here fail to reveal any molecular detail on the DNA surface. Sharper styli than those used here might be necessary to overcome this limitation, and thus, alternative methods to generate them will become a crucial challenge in the further development of this technique. However, other

factors may ultimately play a role in the resolution attainable by SFM, such as the state of hydration of the DNA molecules, since the presence of a bound layer of water might screen the molecular detail, even if sharper tips are used.

DNA is highly hydrated in solution (Hearst & Vinograd, 1961; Hearst, 1965; Falk et al., 1962, 1963; Wolf & Hanlon, 1975) and can be described in terms of three discrete layers representing primary, secondary, and tertiary hydration shells (Saenger, 1984). Although little experimental data exist on the effect of varying humidity on DNA hydration, the difference of binding energy predicted for solvent molecules bound to the phosphates and to the minor and major grooves (Clementi & Corongiu, 1979a,b, 1980; Corongiu & Clementi, 1981) suggests that different domains of the molecules could become exposed and accessible to the SFM stylus at different degrees of hydration. Moreover, the interaction between the stylus and the hydrated macromolecule might depend on the hydrophobicity of the probe. Hydrophobic tips might induce local displacement of the water of hydration and expose the macromolecular surface, at the expense of increased surface tension effects. Conversely, hydrophilic styli might be operable at lower forces but may lead to poorer resolution in air.

Testing these or alternative interpretations will become important in the immediate future, as the potential of the scanning force microscope to image reliably biological molecules and assemblies is further established.

ACKNOWLEDGMENTS

We gratefully acknowledge the preparation of DNA plasmids, fragments, and complexes by Mike Reddy and Steve Weitzel.

REFERENCES

Akama, Y., Nishimura, E., Sakai, A., & Murakami, H. (1990) *J. Vac. Sci. Technol., A 8*, 429–433.

Binnig, G., Quate, C. F., & Gerber, Ch. (1986) *Phys. Rev. Lett. 56*, 930–933.

Clementi, E., & Corongiu, G. (1979a) *Biopolymers 18*, 2431–2450.

Clementi, E., & Corongiu, G. (1979b) *Gazz. Chim. Ital. 109*, 201–205.

Clementi, E., & Corongiu, G. (1980) *J. Chem. Phys. 72*, 3979–3992.

Corongiu, G., & Clementi, E. (1981) *Biopolymers 20*, 551–571.

DeLange, A. M., Reddy, M., Scraba, D., Upton, C., & McFadden, G. (1986) *J. Virol. 59*, 249–259.

Engel, A. (1991) *Annu. Rev. Biophys. Biophys. Chem. 20*, 79–108.

Falk, M., Hartman, K. A., Jr., & Lord, R. C. (1962) *J. Am. Chem. Soc. 84*, 3843–3846.

Falk, M., Hartman, K. A., Jr., & Lord, R. C. (1963) *J. Am. Chem. Soc. 85*, 387–391.

Hansma, H. G., Weisenhorn, A. L., Gould, S. A. C., Sinsheimer, R. L., Gaub, H. E., Stucky, G. D., Zaremba, C. M., & Hansma, P. K. (1991) *J. Vac. Sci. Technol., B 9*, 1282–1284.

Hansma, P. K., Elings, V. B., Marti, O., & Bracker, C. E. (1988) *Science 242*, 209–216.

Hearst, J. E. (1965) *Biopolymers 3*, 57–68.

Hearst, J. E., & Vinograd, J. (1961) *Proc. Natl. Acad. Sci. U.S.A. 47*, 825.

Keller, D., & Chih-Chung, C. (1991) *Surf. Sci.* (in press).

Lazinski, D., Grzadzielska, E., & Das, A. (1989) *Cell 59*, 207–218.

Lee, K. L., & Hatzakis, M. (1989) *J. Vac. Sci. Technol., B 7*, 1941–1946.

Levin, J. R., Krummel, B., & Chamberlin, M. J. (1987) *J. Mol. Biol. 196*, 85–100.

Lindsay, S. M., Nagahara, L. A., Thundat, T., Knipping, U., Rill, R. L., Drake, B., Prater, C. B., Weisenhorn, A. L., Gould, S. A. C., & Hansma, P. K. (1989) *J. Biomol. Struct. Dyn. 7*, 279–287.

Persson, B. N. J. (1987) *Chem. Phys. Lett. 141*, 366–368.

Pilet, J., & Brahms, J. (1972) *Nature, New Biol. 236*, 99–100.

Rugar, D., & Hansma, P. K. (1990) *Phys. Today 43*, 23–30.

Saenger, W. (1984) in *Principles of Nucleic Acid Structure* (Cantor, C., Ed.) Springer-Verlag, New York.

Vesenka, J., Tang, C. L., Guthold, M., Keller, D., & Bustamante, C. J. (1992) *Ultramicroscopy* (in press).

Weisenhorn, A. L., Hansma, P. K., Albrecht, T. R., & Quate, C. F. (1989) *Appl. Phys. Lett. 54*, 2651.

Weisenhorn, A. L., Gaub, H. E., Hansma, H. G., Sinsheimer, R. L., Kelderman, G. L., & Hansma, P. K. (1990) *Scanning Microsc. 4*, 511–516.

Whalen, W., Ghosh, B., & Das, A. (1988) *Proc. Natl. Acad. Sci. U.S.A. 85*, 2494–2498.

Wolf, B., & Hanlon, S. (1975) *Biochemistry 14*, 1661–1670.

Zasadzinski, J. A. N., Helm, C. A., Longo, M. L., Weisenhorn, A. L., Gould, S. A. C., & Hansma, P. K. (1991) *Biophys. J. 59*, 755.